JOURNAL INDIAN ASSOCIATION OF SEDIMENTOLOGISTS ISSN NO 2582 – 2020
Vol. 38, Issue 1, 2021, pp. 75-92
DOI: https://doi.org/10.51710/jias.v38i1.181

Provenance Characterization and Palaeoenvironmental Analysis of the Meta-Sedimentary Rocks of Sonaghati Formation, Betul District, Madhya Pradesh Using Geochemical Approach

Shradha Shukla[1]*, Biswajeet Lenka[2], Hemraj Suryavanshi[3], Subhrasuchi Sarkar[1]
[1]Geological Survey of India, SU: Madhya Pradesh, Bhopal.
[2] Geological Survey of India, SU: Orrisa, Bhubaneshwar.
[3] Geological Survey of India, NMH-II, Nagpur
* Corresponding author email: shradha.sukla@gsi.gov.in.

Abstract

Betul belt, ENE-WSW trending, 135 km long, prominent litho-tectonic unit exposed in the central part of Central Indian Tectonic Zone (CITZ) is composed of meta-sedimentary & meta-volcanic rocks intruded by mafic-ultramafic and granitic suite of rocks, belonging to Palaeoproterozoic to Neoproterozoic age. This belt is traversed by several ENE-WSW trending, sub-vertical ductite shear zones.

The meta-sedimentary rocks of Sonaghati Formation were geochemically characterized and their geochemical composition was interpreted for provenance characterization and paleo-environmental assessment. The weathering indices including Chemical index of Alteration, Chemical index of Weathering, Plagioclase Index of Alteration and Weathering Index of Parker indicate that theses meta-sedimentary rocks have witnessed the substantial amount of weathering at the source without any evidence of potash metasomatism. The Bivariate plots using the major and trace element composition show co-linear trends, which reflect that all these samples belong to co-genetic population and the visible compositional variation could be attributed to chemical, mineralogical and textural maturity.

The Sonaghati metasedimentary rocks are enriched in REE with negative Eu anomaly. The LREE enrichment varies from 122 to 174 times and that of the HREE enrichment ranges from 12 to 31 times of Chondrite indicating highly varied protoliths. The provenance characterization was attempted using the large ion lithophile elements and high field strength elements. The results show that the precursor for these meta-sedimentary litho-units are mixed source with the major contributor being felsic to intermediate and minor contribution has come from the mafic end members. These meta-sedimentary rocks were deposited in the overall semi arid climate with a sequential transition, suggesting the variable climatic conditions ranging from semi-arid to arid. The Cu/Zn, V/Cr ratios, and presence of pyrites dissemination and stringers eventually indicate the prevalence of reducing environmental conditions during the deposition of these meta-sediments.

Key words: *Betul Belt, Meta-Sedimentary, Geochemistry, Graphite, Central Indian Tectonic Zone*

Introduction

The paleo-environmental reconstruction and characterization for understanding the ancient geological architecture is always enigmatic. The geochemistry is one of the classical tools having wide acceptability and ubiquitous applicability in deciphering the past geological processes. Nearly 70% of the global sedimentary mass is made up of the fine grained terrigenous sediments (Garrels and Mackenzie, 1971; Taylor and McLennan, 1985), therefore the geochemical characterization of these sediments can eventually provide the synoptic understanding about the overall crustal composition and subsequently after eliminating the effects of weathering and metamorphism the provenance characterization can also be attempted. (Nesbitt and Young, 1982, 1984, 1989; Hayashi et al., 1997)

The Betul belt, is ENE-WSW trending, 135 km long, prominent litho-tectonic unit exposed in the central part of Central Indian Tectonic Zone (CITZ). Its northern limit is defined by Son- Narmada South Fault (SNSF) and southern limit by Gavilgarh Tan Shear zone (GTS). Predominantly, Betul belt is composed of meta-sedimentary and meta-volcanic rocks intruded by mafic-ultramafic and granitic suite of rocks, belonging to Palaeoproterozoic to Neoproterozoic age (Srivastava and Chellani, 1995). The latest detailed tectono-stratigraphy of the Betul belt after Chakraborty et al. (2009) is given in the Table 1.1. The base-metal

mineralization is hosted within the meta-volcanic rocks whereas, the graphite mineralization is mainly concentrated within the meta-sedimentary rocks (GSI Bulletin series A-69, 2018).

Table1.1: The tectonostratigraphic succession of Betul belt (after Chakraborty et al., 2009)

DECCAN TRAPS	Basaltic lava flows and dolerite dykes	
Intrusive contact / Disconformity		
GONDWANA SUPERGROUP	Conglomerate, sandstones, and shales	
Unconformable / Tectonic Contact		
BETUL GROUP	INTRUSIVES	Basic dykes, pegmatites, quartz veins, homophanous amphibole-mica granite, porphyritic granite
	Intrusive / Tectonic contact	
	PADHAR MAFIC – ULTRAMAFIC SUITE	Diorite, epidiorite, gabbro, norite, pyroxenite, hornblendite, websterite, harzburgite, anorthosite, diorite, talc – serpentinite rock, quartz – epidote rock
	Intrusive / Tectonic contact	
	SONAGHATI FORMATION	Intercalated sequence of quartzite, quartz-mica schist and graphite schist
	Conformable / Tectonic contact	
	BARGAON FORMATION	Meta-sediments (mica schists), meta-rhyolite and felsic metatuff, metabasalt and amphibole – chlorite schist
	Conformable / Tectonic contact	
	RANIPUR FORMATION	Phyllite, banded hematite / magnetite quartzite, BIF, granulite, meta-basalt, amphibolites, carbonaceous phyllites, calcareous quartzite, calc-silicates, marble
Un-conformable / Tectonic contact		
AMLA GNEISS	BASEMENT ROCK	Banded migmatite gneiss, Quartzo-feldspathic mica schist /gneiss

The geochemical characterization of different litho-units of Betul Supracrustal rocks has been earlier attempted (Alam et al., 2009; Mishra et al., 2011; Praveen et al., 2016; Yousuf et al., 2019) but till date the metasedimentary rocks including the quartz mica schist and graphite schist of the Sonaghati Formation have neither been geochemically characterized nor interpreted in detail for provenance and depositional environment delineation. In the present study the geochemical characterization of meta-sediments of the Sonaghati Formation exposed in the Tikari-Gauthana-Chiklar area, Betul district, was attempted for provenance delineation. The samples of Graphite schist and Quartz Mica Schist were geochemically analyzed and interpreted. Considering the limited extent of disposition and the mono-mineralic nature of the quartzite band inter-bedded with the quartz mica schist; the quartzites were not utilized in the synoptic interpretation of plaeoarchitecture.

Geology

The Tikari-Gauthana-Chiklar area is located in the western part of Betul belt, which extends from Chhindwara in the east to Chicholi in the west in the ENE-WSW direction (Fig.1). The Betul belt is traversed by several ENE-WSW trending, sub-vertical ductile shear zones and the NE-SW trending Sonaghati Shear Zone is one of the prominent one running across the present study area. The Sonaghati Shear Zone separates the metasedimentary rocks exposed in the western and northwestern part from the bimodal volcano-sedimentary rocks exposed in the eastern and central parts of Betul belt (Chakraborty et al., 2009). The Tikari-Gauthana-Chiklar area exposes the basement Granite Gneisses with amphibolites and the meta-sedimentary package including Quartz Mica Schist (QMS), Graphite Schist (GS) and Quartzite belonging to Sonaghati Formation. These are intruded by multiple generations of pegmatite, and quartz veins.

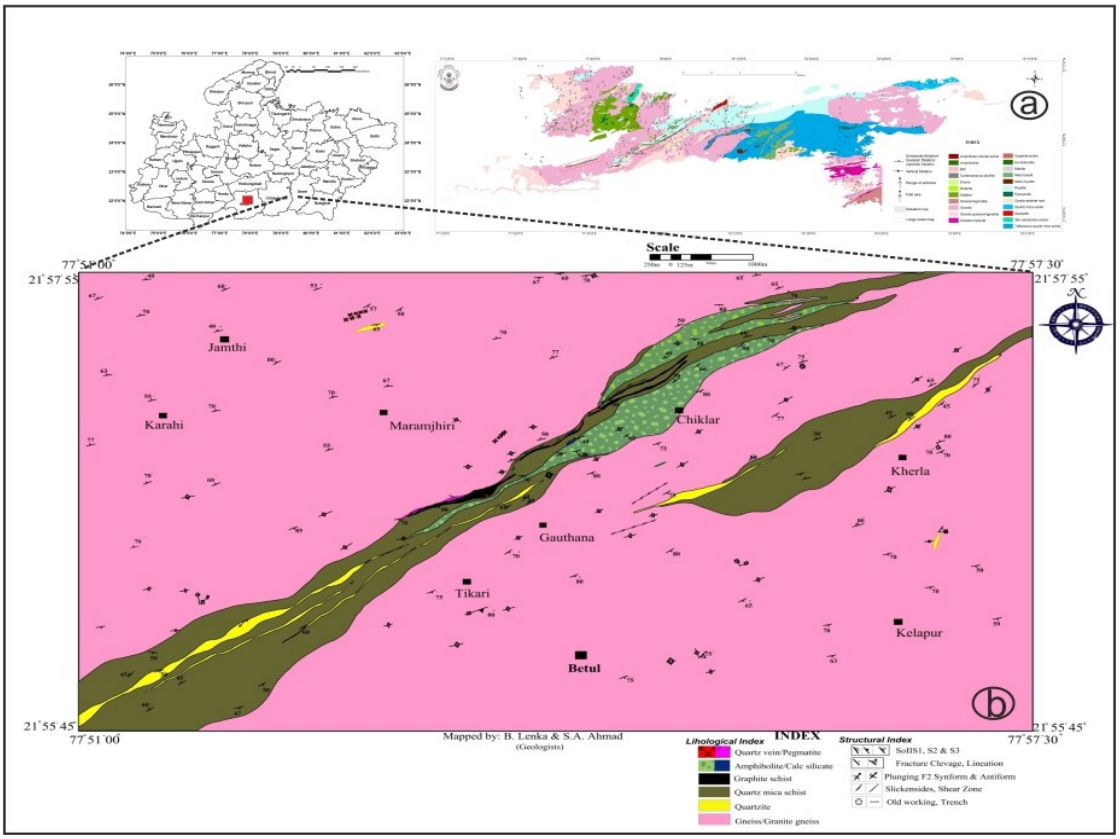

Fig.1: Regional Geological Map of Betul belt showing the location of Tikari-Gauthana-Chiklar area, Betul district (Inset: District Map of Madhya Pradesh showing the location of Betul district). b) Large Scale Map on 1:12,500 scale of Tikari, Gauthana and Chiklar and surrounding areas Betul district (after Lenka & Ahmad, 2013)

Although these intrusive rocks from the present study area were not studied for systematic geochronlogical studies, till date but one of the post-tectonic granitic phases in the vicinity has yielded a Rb–Sr age of ca. 850 ± 50 Ma (Sarkar, 1986; Raut and Mahakud, 2002; Roy and Prasad, 2003), which constrains the upper age of Betul supracrustal sequence. The secondary calcite veins are also recorded (Lenka and Ahmad, 2013).

Megascopically, the QMS is fine to medium grained, thinly foliated, with S0 parallel S1 and exposed as continuous band having the strike of ENE-WSW and vertical to sub vertical dip with variable direction. The dominant mineral phases are quartz, sericite, muscovite, biotite and chlorite with some epidote and ± garnet (Lenka and Shukla, 2016). The discontinuous lensoidal quartzite bands, inter-bedded with micaceous quartzite and QMS having the gradational contact with each other are also recorded at some places. This lithological variation within the meta-sedimentary package in limited areal extent is attributed to the mineralogical disparity within the precursor lithology of each litho-unit. The lensoidal inter-banding of quartzite within the QMS showing pinching and swelling (Fig. 2a) nature is developed during two phases of deformation (Lenka, 2014), due to different rheological properties of these litho-units. The evidences of two generations of folding were also observed within this QMS (Lenka, 2014). The GS is exposed in lenticular discontinuous bodies disposed in an en-echelon pattern over a strike length of 3.5 km within the QMS. In the present study area three bands of GS (5 m to 135 m wide) have been identified by Lenka and Ahmad (2013) (Fig.1b).

Megascopically, the GS is black to steel grey in color, fine to medium grained, soft, greasy and schistose with closely spaced foliation defined by parallel alignment of mica and graphite flakes (Fig. 2b). The dominant minerals include flaky and amorphous graphite, quartz, muscovite and feldspars in varying proportions. The lensoidal and pinching - swelling behavior of the graphite bearing bands and intermittent quartzo-feldspathic siliceous partings has been recorded within GS by Lenka and Shukla (2016). The evidences of shearing and three generations of folding are also well preserved (Fig. 2 c, d). The F_1 folds are tight isoclinals and rootless in nature whereas the F_2 and F_3 are tight to open, inclined with moderate to steep plunge (Lenka and Ahmad, 2013). The later intrusive calcite and quartz veins with mm to cm thickness were recorded in the outcrop and thin sections.

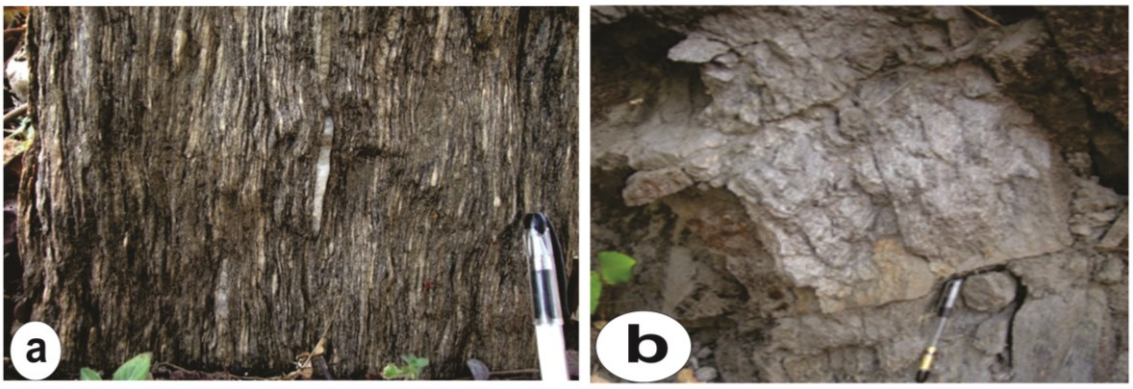

Fig. 2 (a) The field photograph of QMS, north of Sonaghati ridge, Sonaghati area (21°55′57′′N 77°53′13′′E) showing well developed schistocity and stretched and flattened quartz grains along the schisoticty plain. (b) The field photograph of Graphite Schist exposed in an old working north of Tikari village (21°55′42′′N 77°53′17′′E).

Fig. 2 (c) The field photograph of F_2 folds enveloped by F_3 warps in GS exposed in NW of Chiklar village (21°56′46′′N; 77°54′38′′E). (d) The field photograph of F_2 folding in quartzite plunging SW exposed in north of Gauthana village (21°56'12"N; 77°53'53"E).

Material & Methodology

The current study forms a part of the annual field season program of Geological Survey of India (GSI), G2 Stage exploration for graphite in Tikari-Gauthana-Chiklar block, Betul district for establishing the strike and depth continuity and resources augmentation. The petrochemical characterization of the host and the associated lithounits was also carried out for better understanding of the geological setup and the mineralization. In the present study sixteen randomly selected core samples of different meta-sedimentary rock units including GS and QMS from varying depths were selected for geochemical characterization from Sonaghati Formation of the Betul belt. The due care was taken for homogeneous and true representation of the rock formations. The samples were collected from 06 boreholes, with the sample depth ranging from 100.50 m to 209.70 m below the surface (Table 2). Another factor considered during samples selection was the fixed carbon content. These samples were selected in such a way that the overall chemical variation of the major and trace elements with reference to the fixed carbon content (ranging from 0 to 18.50 %) could be determined and interpreted.

The collected samples were pulverized up to 120-mesh size following the standard procedure of sample processing for petrochemical analysis of the GSI (SOP GSI, 2010) and all the adequate precautions were adapted to avoid anthropogenic contamination. These samples were analyzed using the M/S Analytical, X-Ray Fluorescence Spectrometer at Chemical Laboratory, GSI, SR, Hyderabad for major and trace elements. The precision of XRF for major oxide data is ± 5 % and that of trace element data is ± 10%. The standards GSR-1M were used for routine calibration and quantification. The analysis for fixed carbon content and the volatile matter was carried out at Chemical Lab, Bhopal using Atomic Absorption Spectrophotometer - Graphite Furnace of Varian make model no. AA-220, instrument. The precision of AAS for fixed carbon analysis is ± 2 %. Out of the 16 samples, 05 samples were analyzed for rare earth

Table: 2: The Analytical results of Major and Trace Elements for the samples of meta-sedimentary from, Sonaghati Formation

Sample No.	PCS-3	PCS-7	PCS-11	PCS-12	PCS-13	PCS-14	PCS-15	PCS-16	PCS-17	PCS-18	PCS-19	PCS-20	PCS-21	PCS-22	PCS-23	PCS-24
Rock Type	Quartz Mica schist	Quartz Biotite schist	Graphitic schist	Graphitic schist	Graphitic schist	Graphitic schist	Graphitic schist	Graphitic schist	Graphitic schist	Graphitic schist	Graphitic schist	Graphitic schist	Graphitic schist	Graphitic schist	Graphitic schist	Graphitic schist
Borehole No.	BBT-11	BBT-12	BBT-08	BBT-08	BBT-08	BBT-09	BBT-09	BBT-09	BBT-11	BBT-11	BBT-12	BBT-12	BBT-13	BBT-13	BBT-14	BBT-14
Sample depth	100.50m	209.70m	122.90m	132.10m	187.30m	135.7	154.00m	164.70m	123.80m	133.55m	158.00m	188.25m	150.50m	157.90m	156.00m	163.10
FC (%)	0	0	0.45	7.82	13.73	0.78	13.51	8.17	0.53	8.03	10.92	18.5	1.6	9.41	3.35	16.08
SiO2 (%)	64.07	59.50	69.62	63.86	75.26	68.77	68.74	68.53	67.28	68.82	68.57	64.98	62.38	72.25	64.07	69.20
Al2O3 (%)	8.37	13.96	11.75	16.71	12.25	10.00	13.59	14.44	12.47	14.17	12.37	17.55	16.04	13.89	18.84	15.72
Fe2O3 (%)	14.81	7.91	8.38	7.86	4.59	8.25	4.40	6.70	11.57	8.16	6.40	5.00	9.48	3.56	5.57	5.44
MnO (%)	0.83	0.52	0.76	0.21	0.06	0.63	0.12	0.20	0.52	0.24	0.16	0.13	0.43	0.12	0.21	0.16
MgO (%)	6.35	9.14	3.63	4.19	2.47	3.65	5.14	3.69	3.23	3.96	3.25	3.10	4.97	4.37	3.49	3.24
CaO (%)	1.31	2.64	1.42	1.33	0.87	5.79	2.16	1.63	1.08	0.38	5.67	2.85	2.35	1.66	1.63	1.38
Na2O (%)	0.97	1.60	0.94	1.00	0.83	0.51	1.47	0.78	0.73	0.80	0.21	0.73	0.42	0.22	0.89	0.76
K2O (%)	2.17	3.66	2.75	4.08	3.13	1.80	3.75	3.47	2.20	2.88	2.74	4.63	2.75	3.23	4.63	3.08
TiO2 (%)	0.54	0.91	0.62	0.61	0.43	0.50	0.47	0.47	0.72	0.51	0.45	0.63	0.59	0.52	0.53	0.53
P2O5 (%)	0.58	0.16	0.14	0.15	0.11	0.10	0.17	0.08	0.19	0.09	0.18	0.41	0.59	0.18	0.15	0.49
Ba (ppm)	1102	715	1304	693	661	705	608	1185	1022	945	323	961	850	653	575	530
Ga (ppm)	5.9	18	8.7	<5	19	<5	15	17	7.9	9.0	15	14	<5	18	19	14
Sc (ppm)	53	26	24	44	29	<3.5	13	28	36	36	6.9	34	20	26	28	24
V (ppm)	157	81	269	758	1108	254	1309	636	261	746	1586	1848	281	1610	317	1411
Th (ppm)	<4	<4	<4	<4	<4	<4	<4	<4	<4	<4	<4	<4	8.3	<4	<4	<4
Pb (ppm)	33	<2	<2	<2	<2	15	<2	<2	44	19	74	<2	51	<2	<2	20
Ni (ppm)	46	66	60	171	145	51	177	119	49	132	299	155	98	234	88	171
Co (ppm)	22	15	16	7.0	14	8.4	8.1	22	21	6.4	23	7.7	14	9.8	9.7	7.1
Rb (ppm)	78	233	117	128	96	81	196	127	112	106	98	154	106	116	185	120
Sr (ppm)	57	121	65	81	96	75	131	74	68	73	65	113	62	62	77	77
Y (ppm)	6.3	21	18	30	31	19	45	28	16	27	45	49	36	49	28	34
Zr (ppm)	86	196	109	156	145	84	139	138	105	116	91	137	121	133	124	131
Nb (ppm)	20	30	22	19	7.5	22	17	19	22	23	23	19	25	20	52	22
Cr (ppm)	98	163	139	259	298	123	367	241	122	272	455	629	140	526	161	438
Cu (ppm)	98	12	94	258	444	79	577	423	149	363	916	322	249	604	173	423
Zn (ppm)	98	66	117	312	625	79	334	227	98	285	767	155	293	694	179	364
CIA	65.28	63.87	69.71	72.27	71.72	55.23	64.84	71.06	75.67	77.76	58.93	68.14	74.40	73.11	72.51	75.05
ICV	3.22	1.89	1.57	1.15	1.01	2.11	1.29	1.17	1.61	1.19	1.53	0.97	1.31	0.98	0.90	0.93
CIW	78.60	76.71	83.28	87.74	87.79	61.32	78.94	85.69	87.32	92.36	67.76	83.08	85.29	88.10	88.22	87.99
WIP	3184.17	5234.48	3340.10	4489.93	3377.08	2963.50	4713.73	3868.45	2691.35	3252.32	3481.66	4869.13	3330.09	3435.21	4831.04	3458.54

elements (REE) using the ICP-MS, Perkin Elmer Sciex, model no. ELAN -6100, instrument at Chemical Lab, GSI, Nagpur following the standard procedure of analysis with the accuracy and precision of ± 5 %. The four samples were analyzed at Mineral Physics Laboratory, GSI, CR, Nagpur using the XRD instrument for identification of minerals. The sampling and analytical details are given in Lenka and Shukla (2016).

Results

Petrography

The GS and QMS are fine grained rocks with equigranular hypidiomorphic texture. The dominant mineral phases in QMS are muscovite, quartz and opaques (graphite/ Fe-Ti oxides) whereas chlorite, k-feldspar, plagioclase, biotite, hornblende and diopside occur in minor proportions with variations in samples. The kyanite and andalusite are also present in traces. The above-mentioned minerals also occur in GS. In addition these rocks also contain flaky amd amorphous type of graphite. Muscovite/ biotite occur as tabular elongated grains and define the schistosity (Fig.3a-b), whereas quartz occurs as anhedral grains with equigranular interlocking granoblastic texture. Quartz shows undulose extinction and stretched quartz grains define the schistosity. Graphite occurs along the foliation planes as isolated, flat, plate-like minerals. It also occurs as irregular or angular crystalline flakes and, as opaque anhedral to cryptocrystalline globular porphyroblasts (Fig. 3e-f).

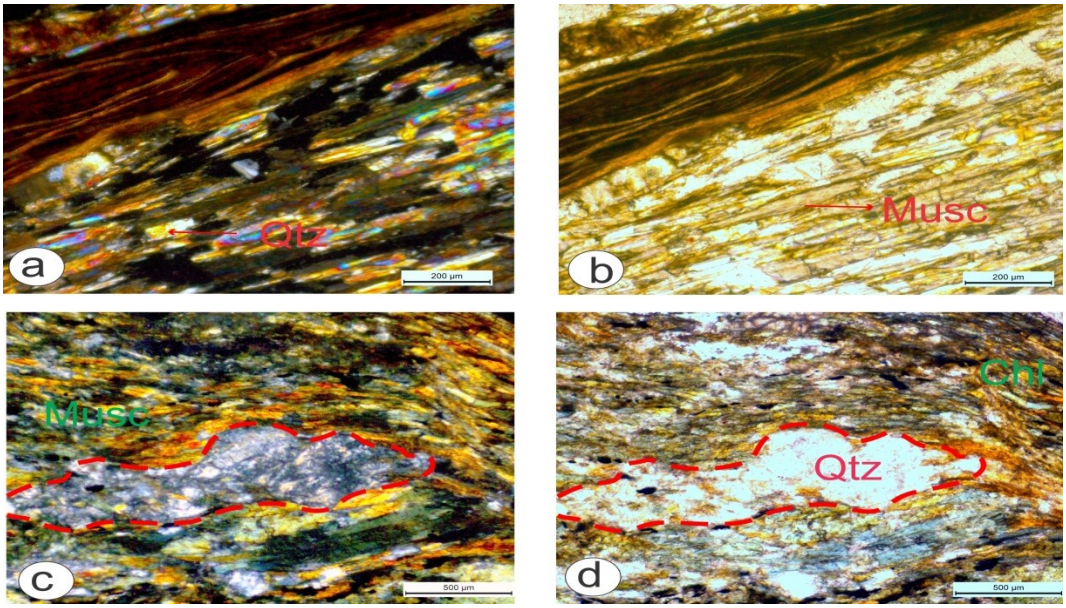

Fig.3 (a & b): Photomicrograph of Quartz Mica Schist with prophyroblasts having flow banding typical aligned along the dominant schistosity defined by quartz and muscovite (c & d): Photomicrograph of Quartz Mica Schist with pinching and swelling of Q domain along the dominant schistosity.

The schistosity is well developed and defined by parallel alignment of graphite flakes (Fig. 3e-f & Fig. 4a), biotite and muscovite. Both Q-domain and M-domain can be identified (Fig. 3g-h) in the thin sections. The M-domain is dominantly composed of tabular micaceous grains and graphite with occasional presence of quartz whereas; Q-domain is defined mainly by quartz with small amount of mica in the inter-granular spaces. In some cases, typical granoblastic texture is observed along with the development of triple junctions. Evidence of shearing is depicted by pinch and swell structure (Fig. 3c-d) and presence of mica fish. The lithic fragment (rhyolite?) is observed in thin section of QMS (Fig. 3a-b).

XRD Studies

The four surface samples of GS from Tikari-Gauthana-Chiklar area, were analyzed using the XRD for mineral identification. The major minerals identified were quartz (45% to 57%), muscovite (25% to 40%), montmorillonite (0 to ~16%), clinochore (0 to ~15%), graphite (3% to 4%), calcite (0 to ~15%), nontronite (0 to ~10%), and kanemite (0 to ~2%) (Fig.4b; Table 3).

Major Oxides

The detailed geochemical analytical results of the samples of Graphite Schist and Quartz Mica Schist of Sonaghati Formation are presented in Table 2. The SiO_2 content in the analyzed samples varies from 59.50% to 75.26% and the Al_2O_3 varies from 8.37% to

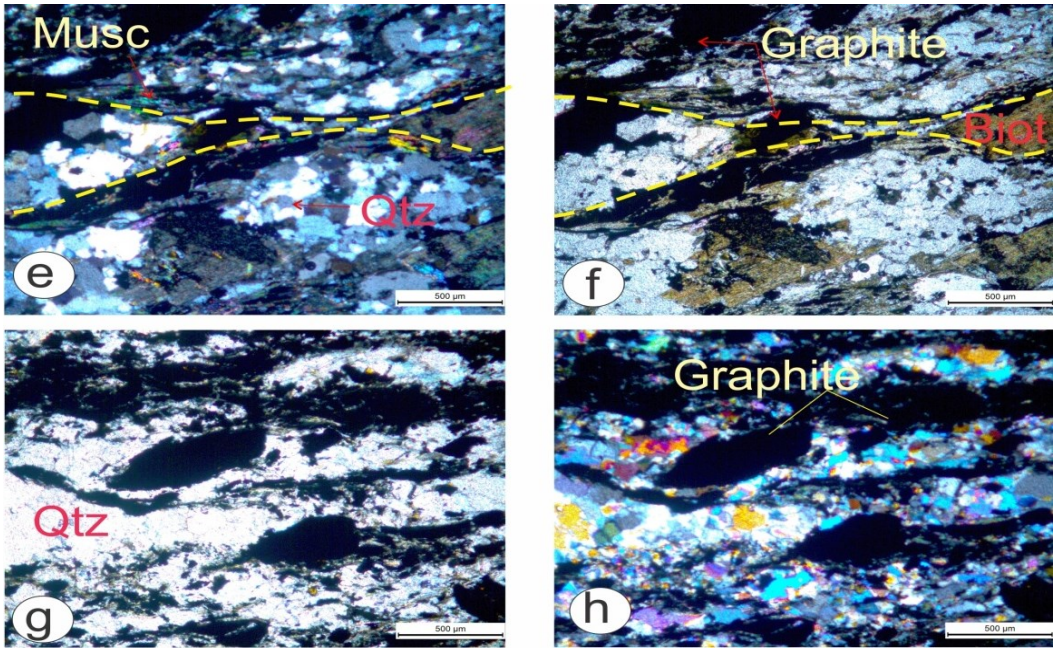

Fig.3: (e & f): Photomicrograph of Graphitic Schist with alternate Q and M domains, pinching and swelling is also observed. (g & h): Photomicrograph of Graphitic Schist with alternate domains of quartz rich layer and graphite rich layers. The graphite flaks is distinctly observed. (PPL and cross nicol view- right and left half respectively).

Table1.3. The results of XRD analysis for the samples of meta-sedimentary from, Sonaghati Formation.

Sample No	Rock Type	Location	
GR-01	Graphite Schist	21^0 58' 40.3166" 77^0 54' 30.9045"	Quartz ≈ 45.00%; Muscovite ≈ 35.00%; Montmorelonite ≈ 16.00%; Graphite ≈ 04.00 %
GR-02	Graphite Schist	21^0 56' 23.1230" 77^0 54' 7.2839"	Quartz ≈ 57.00%; Muscovite ≈ 40.00%; Graphite ≈ 03.00 %
GR-03	Graphite Schist	21^0 56' 14.5125" 77^0 53' 50.4474"	Quartz ≈ 55.00%; Muscovite ≈ 27.00%; Clinochore ≈ 15.00%; Graphite ≈ 03.00 %
GR-04	Graphite Schist with Calcite veins	21^0 56' 3.7390" 77^0 53' 22.5696"	Quartz ≈ 45.00%; Muscovite ≈ 25.00%; Calcite ≈ 15.00%; Nontronite ≈ 10.00%; Graphite ≈ 03.00 %; Kanimite ≈ 02.00 %

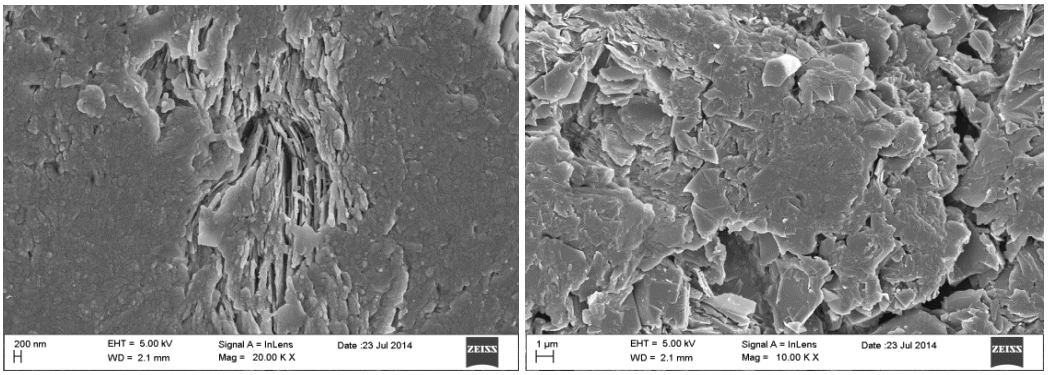

Fig. 4: (a). SEM microphotograph of GS of Tikari-Gauthana-Chiklar area, Betul district showing crystalline elongated graphite with intrinsic flaky morphology along with the shattered grains along the foliation planes.

Table 4: The Correlation Matrix for the samples of meta-sedimentary rocks from, Sonaghati Formation, showing the elemental inter relationship.

	FC (%)	SiO2 (%)	Al2O3 (%)	Fe as Fe2O	MnO (%)	MgO (%)	CaO (%)	Na2O (%)	K2O (%)	TiO2 (%)	P2O5 (%)	Ba (ppm)	Ga (ppm)	Sc (ppm)	V (ppm)	Pb (ppm)	Ni (ppm)	Co (ppm)	Rb (ppm)	Sr (ppm)	Y (ppm)	Zr (ppm)	Nb (ppm)	Cr (ppm)	Cu (ppm)	Zn (ppm)
FC (%)	1.00																									
SiO2 (%)	0.44	1.00																								
Al2O3 (%)	0.39	-0.31	1.00																							
Total Fe as	-0.72	-0.44	-0.52	1.00																						
MnO (%)	-0.83	-0.36	-0.62	0.82	1.00																					
MgO (%)	-0.45	-0.66	-0.16	0.33	0.41	1.00																				
CaO (%)	-0.04	-0.09	-0.22	-0.09	0.09	0.00	1.00																			
Na2O (%)	-0.11	-0.38	0.04	0.09	0.16	0.58	-0.34	1.00																		
K2O (%)	0.47	-0.26	0.83	-0.59	-0.61	0.01	-0.22	0.34	1.00																	
TiO2 (%)	-0.45	-0.67	0.12	0.33	0.42	0.63	-0.10	0.47	0.11	1.00																
P2O5 (%)	0.04	-0.38	0.05	0.37	0.22	0.18	-0.07	-0.13	-0.10	0.09	1.00															
Ba (ppm)	-0.39	-0.09	-0.24	0.52	0.56	0.05	-0.43	0.15	-0.20	0.24	0.08	1.00														
Ga (ppm)	0.38	0.09	0.57	-0.80	-0.70	0.01	0.28	0.00	0.69	-0.12	-0.39	-0.59	1.00													
Sc (ppm)	-0.28	-0.24	-0.15	0.59	0.40	0.12	-0.61	0.19	-0.06	0.22	0.21	0.50	-0.52	1.00												
V (ppm)	0.92	0.47	0.28	-0.71	-0.77	-0.42	0.13	-0.32	0.36	-0.44	0.04	-0.45	0.35	-0.38	1.00											
Pb (ppm)	0.01	-0.30	0.09	-0.01	-0.22	-0.05	0.33	-0.66	0.17	0.01	0.10	-0.35	0.42	-0.62	0.30	1.00										
Ni (ppm)	0.71	0.37	0.25	-0.63	-0.75	-0.30	0.23	-0.40	0.28	-0.47	-0.10	-0.63	0.42	-0.53	0.86	0.56	1.00									
Co (ppm)	-0.39	-0.04	-0.51	0.50	0.40	0.12	0.12	-0.13	-0.42	0.06	0.06	0.31	-0.26	-0.02	-0.29	0.77	-0.12	1.00								
Rb (ppm)	0.07	-0.47	0.51	-0.37	-0.23	0.51	-0.08	0.70	0.71	0.52	-0.19	-0.19	0.51	-0.25	-0.01	0.07	-0.04	-0.25	1.00							
Sr (ppm)	0.41	-0.15	0.26	-0.45	-0.35	0.31	0.04	0.70	0.56	0.27	-0.18	-0.22	0.43	-0.21	0.26	-0.59	0.06	-0.37	0.76	1.00						
Y (ppm)	0.77	0.25	0.52	-0.80	-0.81	-0.28	0.21	-0.32	0.51	-0.34	0.01	-0.52	0.58	-0.61	0.87	0.51	0.83	-0.36	0.21	0.32	1.00					
Zr (ppm)	0.24	-0.27	0.51	-0.43	-0.40	0.44	-0.32	0.58	0.66	0.48	-0.17	-0.15	0.65	-0.05	0.10	-0.16	0.08	-0.30	0.74	0.67	0.25	1.00				
Nb (ppm)	-0.40	-0.54	0.46	0.04	0.11	0.19	0.06	0.09	0.33	0.26	-0.02	-0.17	0.20	-0.05	-0.38	0.29	-0.25	-0.10	0.45	-0.10	-0.15	0.01	1.00			
Cr (ppm)	0.88	0.34	0.36	-0.70	-0.73	-0.32	0.13	-0.29	0.44	-0.28	0.07	-0.40	0.38	-0.33	0.98	0.24	0.81	-0.33	0.09	0.29	0.87	0.19	-0.30	1.00		
Cu (ppm)	0.68	0.51	0.09	-0.57	-0.71	-0.38	0.22	-0.43	0.11	-0.62	-0.12	-0.54	0.34	-0.62	0.80	0.63	0.94	0.06	-0.14	0.00	0.77	-0.08	-0.31	0.71	1.00	
Zn (ppm)	0.55	0.58	0.04	-0.55	-0.65	-0.34	0.12	-0.51	0.04	-0.56	-0.13	-0.61	0.43	-0.50	0.69	0.66	0.88	0.02	-0.25	-0.13	0.67	0.00	-0.33	0.59	0.88	1.00

0.9 Very Significant Correlation (>0.85)
0.75 Significant Correlation (0.65 to 0.85)
0.65 Moderate Correlation (0.50 to 0.85)

18.84%. The proportion of other oxides ranges from 3.56% to 14.81% (Fe_2O_3), 0.43% to 0.91% (TiO_2), 0.06% to 0.83% (MnO), 2.47% to 9.14% (MgO), 0.38% to 5.79% (CaO), 0.21% to 1.60%(Na_2O), 1.80% to 4.63% (K_2O) to 0.08% and 0.59% (P_2O_5).

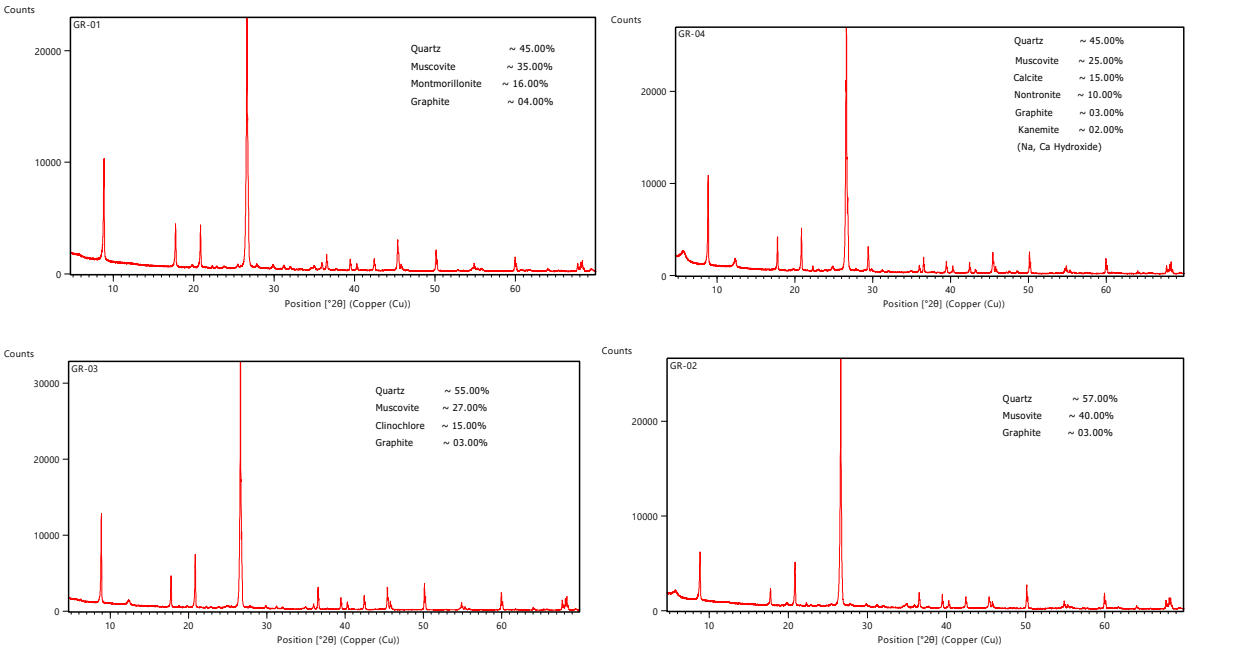

Fig. 4 (b): The XRD results of the samples of Graphite schist of Tikari-Gauthana-Chiklar area, Betul District showing the proportion of major mineral phases.

The bivariate XY plots of major oxides versus SiO_2 wt. % (Fig. 5a) displays a moderate to strong negative correlation between silica and all the other major oxides for all the samples of Sonaghati metasediments except the outlier samples for CaO. The co-linear trends in the XY plots indicate that the elemental characters of GS and QMS are attributed to mineral fractionation and textural maturity. The possible minerals influencing the geochemical signatures are quartz, clay minerals, opaques (Ti-Fe-Mg oxides) and some mafic minerals. The strong positive correlation between Al_2O_3 and K_2O, K_2O and Na_2O suggests the dominance of clay minerals and muscovite (Fig. 5b). The higher concentration of calcium oxide within the outlier sample (PCS-14) is due to the presence of calcite vein, and the same is also validated by petrographic analysis. The sample with calcite vein was selected to understand the variation in bulk rock geochemistry of the meta-sediments after secondary enrichment of calcite and to identify the relation (if any) between REE's, fixed carbon and secondary calcite enrichment in meta-sediments.

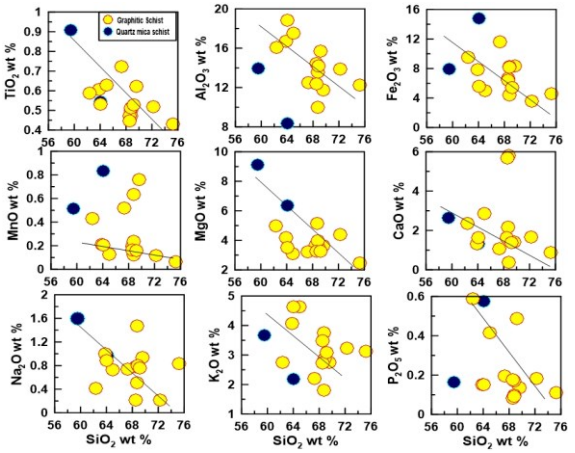

Fig 5 (a) X-Y Variation plots of major oxides with SiO_2 as differentiating index, after Harker.

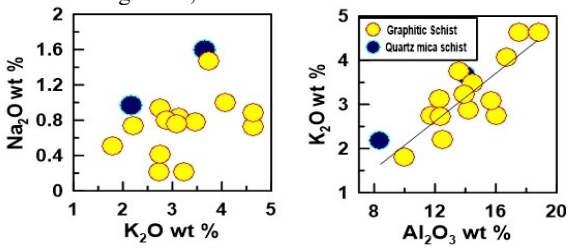

Fig 5 (b). X-Y Variation plots of Na_2O versus K_2O and Al_2O_3 versus K_2O.

The overall assessment of geochemical signatures of outlier sample (PCS-14) suggests that it is having the high concentration for CaO but other elemental association of all the other major oxides and trace elements and REE's are similar with the other samples of meta-sediments. No visible correlation between CaO, REE's, fixed carbon, and other trace elements is recorded (Table 4). The scattered elemental correlation between aluminum and sodium is attributed to the high mobility and low partitioning coefficient of sodium.

The K_2O/Al_2O_3 ratio for the samples of metasediments of Sonaghati Formation ranges from 0.17 to 0.28 with an average of 0.23. This ratio also eventually supplements our inference on the presence of clay minerals (K_2O/Al_2O_3 ratio range = 0.00 to 0.40) (e. g., Cox et al., 1995; Dar et al., 2020).

Trace Elements

A set of trace elements data of the samples of meta-sedimentary units including GS and QMS of Sonaghati Formation is presented in Table 2. The compatible trace elements (Cr, Co, Ni, and V) have a wide range of variations. The concentration ranges (in ppm) are 98 to 629 for Cr, 46 to 299 for Ni, 81 to 1848 for V, 6 to 23 for Co and 12 to 916 for Cu, and 66 to 767 for Zn. In-comparison to the Compatible elements the large ion lithophile elements (LILE's) have restricted abundance range except for barium. The concentration ranges (in ppm) are 78 to 233 for Rb, 57 to 131 for Sr, 323 to 1304 for Ba and <2 to 74 for Pb. The variation of high field strength elements: Y, Sc, Th, U, Zr, Nb and REE's of the GS and QMS of Sonaghati Formation varies from (in ppm) 06 to 49 for Y, 84 to 196 for Zr, 8 to 52 for Nb, for 116.71 to 191.65 for $\sum$ REE and <3.5 to 53 for Sc. The thorium content within all the samples is below detection limit except one sample with 8.3 ppm. The High field strength elements have low mobility and high partitioning coefficient (Taylor and McLennan, 1985), therefore are insoluble and least mobile in the surface conditions.

The multi elemental correlation of the elements elucidates very significant to significant correlation between the fixed carbon, vanadium, chromium, nickel, yttrium, copper and zinc. Another set of elements having the moderately significant correlation among them are sodium, potassium, rubidium, strontium and gallium Table 4.

The binary plots of trace elements (Zr, Cu, Y, V, Ba, Zn and Co) versus nickel are plotted for understanding the effect of mafic and opaque minerals in these elemental abundances. The binary trace element plots of Ni shows a strong positive correlation of Zr, Cu, Y, V and Zn and a moderate negative correlation with Ba and Co (Fig.6a) Along with these, a strong positive relationship between rubidium and strontium is also recorded. These trace element correlations further attenuate the inference derived from the correlation of major oxides that the mineral and textural maturity had impacted the geochemical signatures of these metasediments. Interestingly a strong positive correlation between fixed carbon and vanadium is also noticed. This intricate relationship suggests the possibility for co-genetic organic origin and metamorphic enrichment, of graphite and vanadium mineralization within these meta-sedimentary rocks of Betul belt. The co-linear trends among the compatible elements and high field strength elements suggest that the data set belongs to co-genetic population, eventually uninfluenced by the secondary process of chemical alterations and preserving the primordial elemental signatures.

Rare Earth Elements

The meta-sediments of the Sonaghati Formation are enriched in REE elements with negative Eu anomaly. The LREE enrichment varies from 122 to 174 times and that of the HREE enrichment ranges from 12 to 31 times of Chondrite (Fig..6b, Table 5), indicating highly varied protoliths. For the same group of samples, their $(La/Lu)_N$ varies from ~5.76 to ~14.29 with an average of 9.03, $(La/Sm)_N$ varies from 3.65 to 5.34 with an average of 4.20 and $(Gd/Lu)_N$ varies from 1.00 to 1.70 with an average of 1.44. Thus, the Chond-

Table 5: The Analytical results of Rare Earth Elements for the samples of meta-sedimentary rocks from, Sonaghati Formation

Sample NO	PCS-14	PCS-15	PCS-16	PCS-17	PCS-18
La (pg/g)	41.33	42.49	30.53	28.96	31.66
Ce (pg/g)	75.36	68.57	60.74	59.99	62.78
Pr (pg/g)	8.12	9.63	7.22	6.78	7.41
Nd (pg/g)	30.19	35.37	26.97	25.95	27.02
Sm (pg/g)	5.00	6.67	5.08	5.12	5.11
Eu (pg/g)	1.18	1.40	1.16	1.04	1.23
Gd (pg/g)	4.26	6.41	4.50	4.86	4.75
Tb (pg/g)	0.68	1.08	0.74	0.79	0.76
Dy (pg/g)	3.96	7.15	4.38	5.10	4.86
Ho (pg/g)	0.79	1.59	0.86	0.98	0.90
Er (pg/g)	2.19	4.87	2.41	2.76	2.65
Tm (pg/g)	0.34	0.81	0.38	0.41	0.39
Yb (pg/g)	1.98	4.82	2.21	2.52	2.38
Lu (pg/g)	0.31	0.79	0.37	0.41	0.39
$(La/Lu)_N$	14.29	5.76	8.84	7.57	8.70
$(La/Sm)_N$	5.34	4.11	3.88	3.65	4.00
$(Gd/Lu)_N$	1.70	1.00	1.50	1.47	1.51

rite normalized REE patterns suggests that Sonaghati meta-sediments have much more fractionated LREE's dispersal with nearly flat and enriched HREE's. The presence of strong negative Eu anomaly indicates the Proterozoic age for the precursor of the metasediments. The overall abundance of REE in these meta-sediments is comparable with the North American Shale Composite (NASC) with slight depletion in HREE's except the sample no PCS15. The NASC values are after Gourmet et al. (1984). The sample 'PCS 15' is comparatively more fractionated and displays an enrichment of HREE's in comparison to both Chondrite and NASC (Fig. 6c).

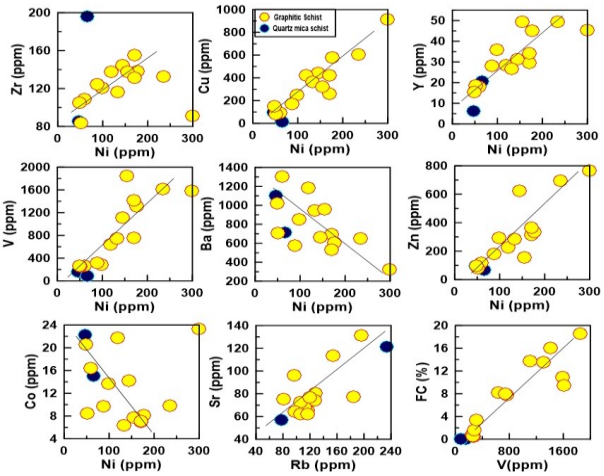

Fig. 6.(a) Variation plots of trace elements { Zircon (Zr), Copper (Cu), Yittrium (Y), Vanadium (V), Barium (Ba), Zinc (Zn), Cobalt (Co)} versus Nickel (Ni); Rubiduim (Rb) versus Srontium; Vanadium (V) versus fixed Carbon).

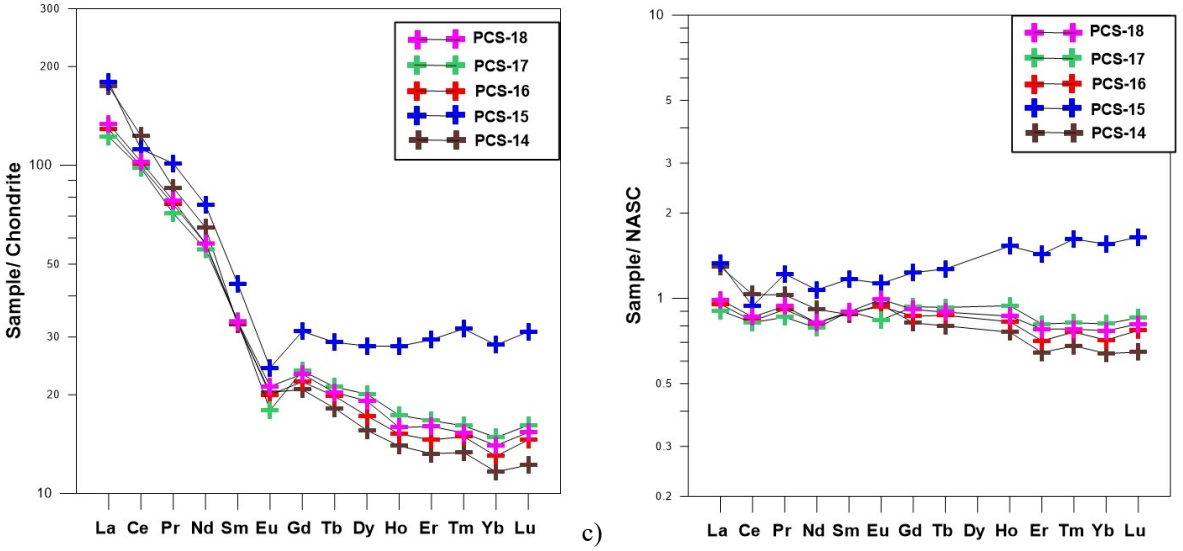

Fig. 6 b) chondrite normalized REE plots for the samples of Tikari-Gauthana-Chiklar area. The chondrite values are after Taylor & MacLennan, 1985. c) The NASC normalized REE plots for the samples of Tikari-Gauthana-Chiklar area.

Indices of Chemical Weathering

The geochemical data processing for understanding the provenance of the meta-sedimentary rocks was carried out. Thus, the chemical weathering indices such as chemical index of alteration (CIA), chemical index of weathering (CIW), plagioclase index of alteration (PIA) and weathering index of parker (WIP) were calculated for the assessment of degree of metamorphism and weathering of the source terrain.

The CIA was calculated using the equation [Al_2O_3 / (Al_2O_3 + CaO + Na_2O +K_2O)] x 100 where all the oxides are in molar proportion and CaO represents Ca in silicate fraction (Nesbitt and Young, 1982, 1984; Fedo et al., 1995; Maynard et al., 1995). The CIA value of all the samples varies from 55.2 to 77.8 with an average of 69.3, is comparable with the average CIA values for global shale (~ 70 to ~ 75) by (Nesbitt and Young, 1982). This range of CIA value indicates the presence of muscovite, illite and smectite within the metasediments of Sonaghati Formation. Theses samples when plotted on the Al_2O_3 – CaO + Na_2O – K_2O (A-CN-K) ternary diagram (Nesbitt and Young, 1984) shows trend sub parallel to A-CN axis, within the limits of weathering and follow the pattern of substantial weathering trend of the source terrain without displaying any evidence of potash metasomatism (Fig.7a).

The Chemical index of Weathering (CIW) (Harnois, 1988) was calculated using the equation [Al_2O_3/ (Al_2O_3+ CaO+ Na_2O)]x100 and the CIW values of all the samples vary from 61.32 to 92.36 with an average of 82.51. The Prince and Velbel (2003) had defined that the CIW values for the unaltered/ fresh samples should be ≤ 50 and that for the optimum weathered samples should be 100. The CIW values for the samples of the present study ranges in between the limits of fresh and optimum weathered samples, with an average value of 82.51. Therefore, considering intermediate CIW values for the meta-sedimentary rocks of Betul belt, it can be inferred that this belt had witnessed the substantial amount of weathering and the elemental data set generated can be effectively utilized for provenance characterization and plaeo-climatic reconstruction.

Prince and Velbel (2003) had also validated the WIP as the most robust indicator with its value 0 for optimum weathered sample and >100 for fresh/ unaltered samples. Parker (1970) introduced the term WIP for silicate rocks. Eswaran et al., (1973) and Hamdam and Bumham (1996) were the pioneer workers involved in assessment and validation of the equation for other litho-units. The WIP values for the samples of the present study was calculated using the equation [(2 Na_2O/0.35) + (MgO/0.9) + (2K_2O/0.25)+ (CaO/0.7)] x 100 (Hamdam and Bumham, 1996). The WIP value for the GS and QMS of Sonaghati Formation ranges from 2691.35 to 5234.48 with an average of 3782.55. This high value of WIP are supportive with our initial inferences that the metasediments of Sonaghati Formation had undergone substantial weathering and are very much suitable for the source area characterization. This index is based on the proportion of the most mobile alkali and alkaline earth metals (sodium, potassium, magnesium and calcium), therefore is most appropriate for evaluation of weathering profile of heterogeneous meta-sedimentary parent rocks (Prince and Velbel, 2003).

The values of all these weathering indices when compared with the sample depth, indicates that CIA and CIW shows an inverse relation and the WIP is having a positive relation with the sample depth. Hence, the degree of alteration in the metasediments of Sonaghati Formation is inversely proportional to the depth (Fig. 7b).

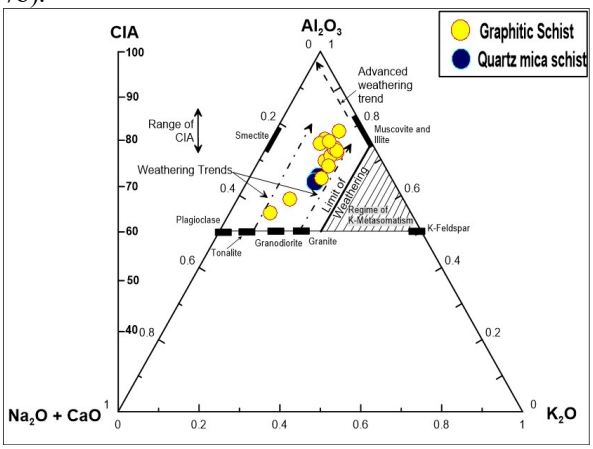

Fig. 7 a) A-CN-K ternary diagram *(after Nesbitt and Young, 1984)* showing weathering trends for the meta-sediments of of Tikari-Gauthana-Chiklar area, Betul District.

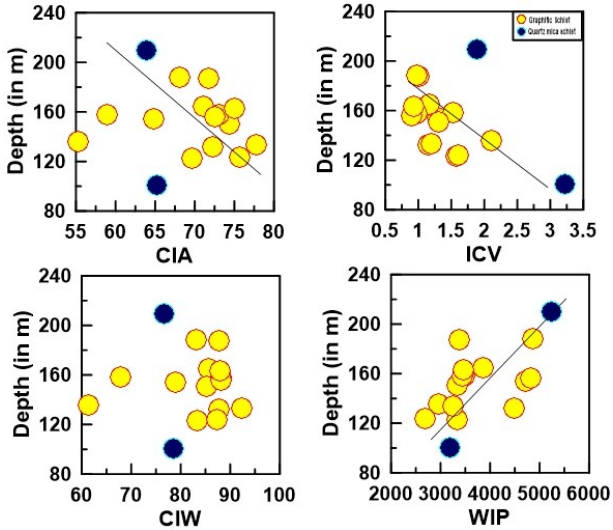

Fig. 7 b) The Bivariate plot of Chemical Weathering Indices (CIA, ICV, CIW and WIP) versus sample depth (in meters) for the meta-sediments of Tikari-Gauthana-Chiklar area, Betul District

Hydraulic Sorting

The index of compositional variability (ICV) after Cox et al. (1995) is useful to ascertain the effect of hydraulic sorting on the geochemical signatures. The

formula used for calculation of ICV is: $Fe_2O_3 + K_2O + Na_2O + CaO + MgO + MnO + TiO_2)/Al_2O_3$. The ICV values for samples from the present study area ranges from 0.90 to 3.22 with an average of 1.43. The figure 6a shows that the ICV had an inverse relationship with the sample depth. The progressive decreasing values of ICV indicate the progressive increase in the degree of hydraulic sorting (Cullers, 2000).

Classification

The Classification of fine clastic meta-sediments using the geo-chemical data has severe limitations but some of the ratio and ternary plots are widely acceptable. The most convenient graphical representation for sedimentary and meta-sedimentary rocks is log weighted ratios of SiO_2 / Al_2O_3 versus (Na_2O+CaO) / K_2O after Garrels and Mackenzie, (1971) and Gilboy (1982). The ratio SiO_2 / Al_2O_3 distinguishes the siliceous sediments from argillaceous sediments whereas (Na_2O+CaO) / K_2O separates the argillaceous from the calcareous. The samples of the present study area fall in the domain of argillaceous pelagic sediments to siliceous ooze (Fig. 8a). These elemental ratios also elucidated that the metasediments of Sonaghati Formation have composition very similar to that of Proterozoic shales. In figure 8b all the samples from the present study are clustered around the average concentration of Proterozoic shale's given by Garrels and Mackenzie (1971). In the diagram showing the relationship between the composition of igneous rocks and those of sedimentary rocks after Garrels and Mackenzie (1971) the samples from the present study shows the scattered dispersion varying between granite- to granodiorite thus suggests that they may have the felsic dominant precursor ranging in composition from granite- to granodiorite (Fig. 8a,b).

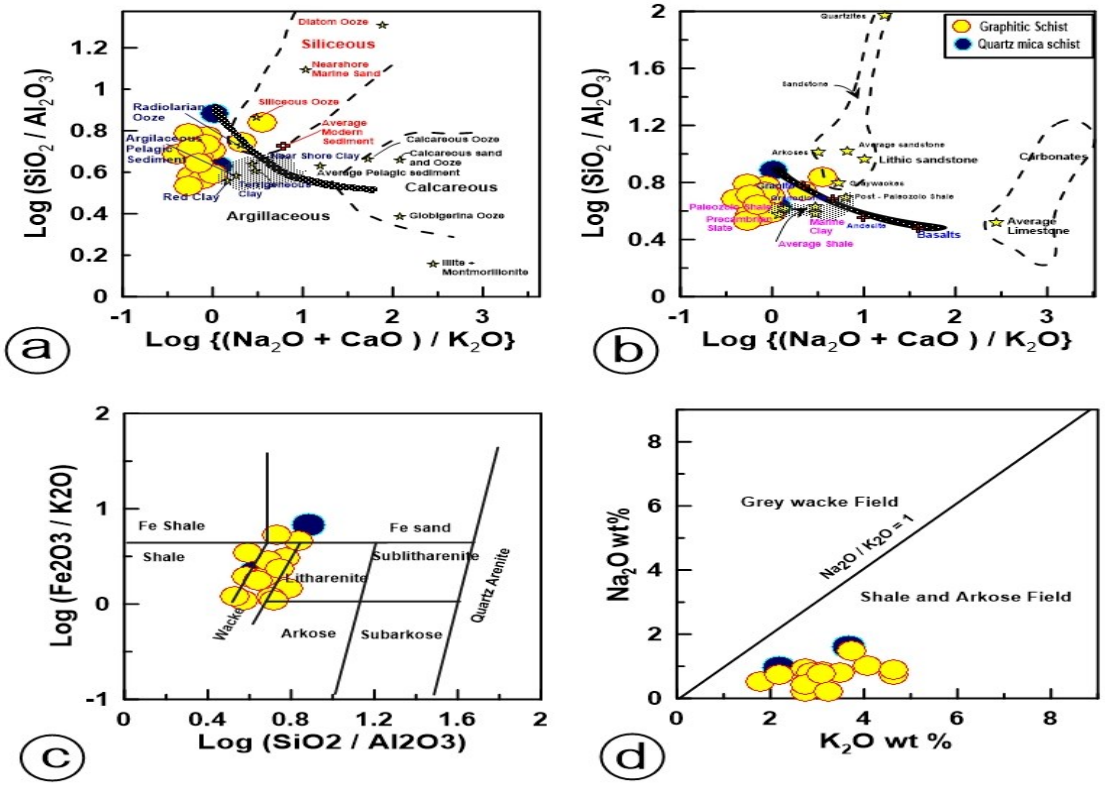

Fig. 8. a) Log SiO_2 / Al_2O_3 vs. (Na_2O+CaO) / K_2O plot (after Garrels and Mackenzie, 1971). (b) Relationship between the composition of igneous rocks and those of sedimentary rocks after Garrels and Mackenzie (1971), The shaded banana shaped area denotes the range of composition of igneous rocks with more silica, sodium, potassium rich rocks to the left grading into magnesium rich rocks to the right. (c) Classification of fine clastics from MSB after Herron (1988). (d) Classification scheme given after *Pettijohn, 1963*

Herron (1988) classification is a scatter diagram of log (Fe_2O_3/K_2O) vs. log (SiO_2/Al_2O_3). This classification system is designed to distinguish subtle composition classes such as sub-arkoses from arkoses and sub-litharenites from litharenites, as well as to distinguish the major sandstone and shale classes. Although the samples of the present study had witnessed the low to medium grade of metamorphism and had lost most sedimentological attributes, but the calculation of weathering indices indicates the

substantial weathering of these rocks. Secondly the chemical signatures of provenance and precursor lithology are still preserved within the detrital grains and other petrographic properties related to sediment maturity within the metamorphic rocks (Culler, 2000; Heinrichs, 2012). Therefore the chemographic scheme given by Herron (1988), Pettijohn (1963) and Gilboy (1982) are utilized for classification of metasediments. In log (Fe_2O_3/K_2O) vs. log (SiO_2/Al_2O_3) (Fig. 8c) bivariate plot the samples of GS and QMS fall in the fields of wacke with some of the samples falling in the border areas of litharenites and shales. These sample have wide variable range of Fe_2O_3/K_2O and the restricted abundance of SiO_2/Al_2O_3.The classification scheme dependent on the total abundance of alkalis (Na_2O and K_2O) given after Pettijohn (1963) and Gilboy (1982) also all the samples fall in the arkosic fields (Fig. 8d).

The sedimentary fractionation tends to concentrate clay minerals and the titanium oxides within the fine clastics and zircon within the coarser components of the same sedimentary suites. Therefore, appreciantly the concentration of Al_2O_3 tends to increase with increasing TiO_2 / Zr within the respective sedimentary system (Gracia et al., 1994). The metasediments pertaining to the present study when projected on the ternary diagram of Al-Ti-Zr after Gracia et al. (1994) gives a clustered appearance. They range in composition form Common shale to Alumina rich shale displaying the progressive chemical transition from the bulk source composition (Fig. 9).

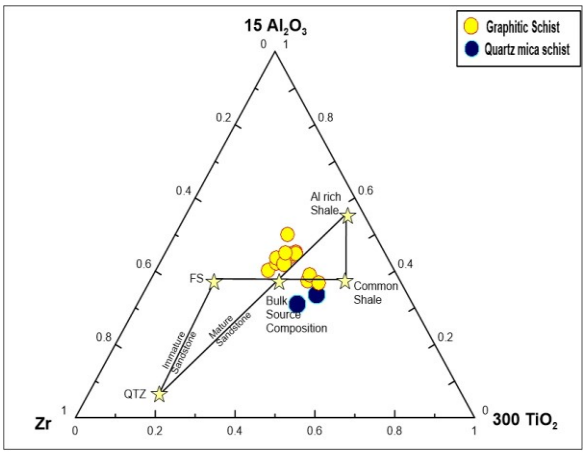

Fig. 9. Classification scheme after Gracia et al. (1994). Model compositions and mixing lines between sandstones and complementary shales are based on an arbitrary bulk source composition. Acronyms: QTZ: quartzite and FS: feldspar rich sandstone.

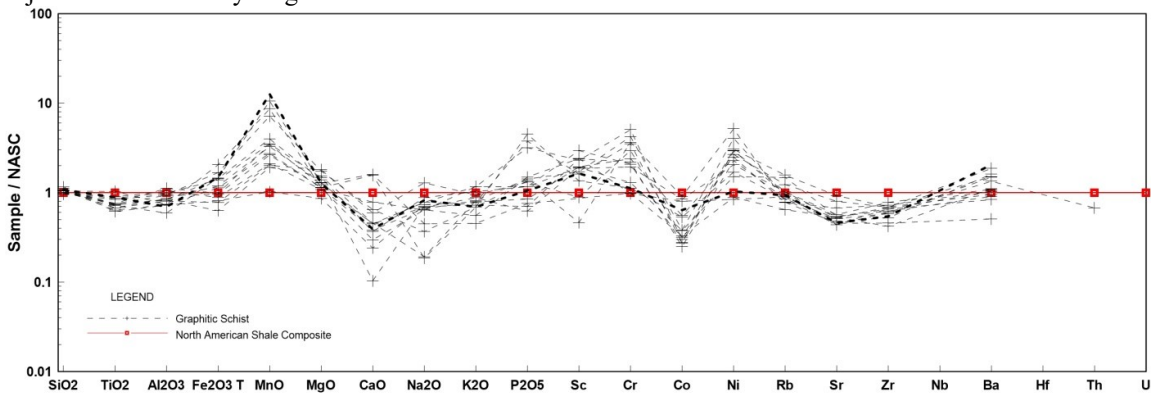

Fig. 10: NASC (North American shale composite)–normalized average major- and trace-element composition of all the samples of graphitic schist. NASC values are from Groumet et al. (1984).

Discussion

The elemental signatures are the keys for understanding the depositional environment and the source composition of the sedimentary rocks. Owing to the fine grained nature of the meta-sediments the major and trace elemental signatures were precisely analyzed and the systematic provenance characterization was attempted using the elements with low partition coefficient between natural water and upper crust and short oceanic residence time. The North American Shale Composite (NASC) normalized multi element diagram indicates that all these samples are comparable with NASC (Fig. 10) but slightly enriched in MnO, P_2O_5, Cr, Sc, Ni and Ba and depleted in CaO, Na_2O, Co, Sr & Zr. The NASC values are after Gourmet et al. (1984).

Provenance

The geochemical characters of a meta-sedimentary litho-assemblage vary as a function of primary and secondary process. The primary processes indicate towards the source characters and the secondary process includes intensity and duration of weathering, sedimentary recycling, digenesis/low grade

metamorphism and sorting. (Swyer, 1986; Wronkiewicz and Condie et al., 1987; McLennan et al., 1993). Various authors have given several elemental relationships for provenance identification and characterization although each has some limitations, but meaningful inferences could be drawn from combined evaluation. In the present study the provenance delineation of the meta-sediments, from Sonaghati Formation, was attempted using the elements having low partition coefficient between natural water, upper crust and short oceanic residence time. One such promising tool is zirconium concentration, when unaffected by sedimentary recycling of quartzose precursor. The average zircon abundance within the samples of our study ranges from 84 to 196 ppm, which actually gives the hunch for felsic-dominated precursor. This assumption was subsequently validated with the TiO_2 (wt. %) vs. Zr (ppm) bivariate plot (Hayashi et al., 1997) and K_2O (wt. %) and Rb (ppm) bivariate plot (Floyd and Leveridge,1987 and Floyd et al., 1989).

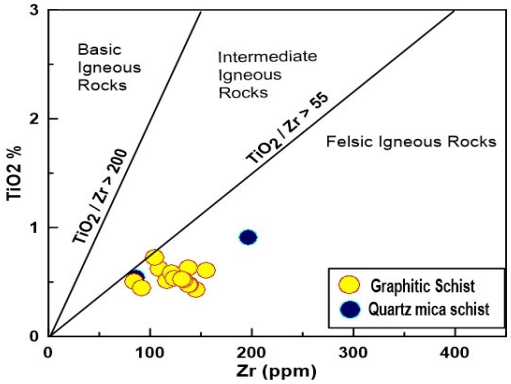

Fig. 11 a) TiO_2 (wt %) versus Zr (ppm) bivariate diagram (after Hayashi et al., 1997).

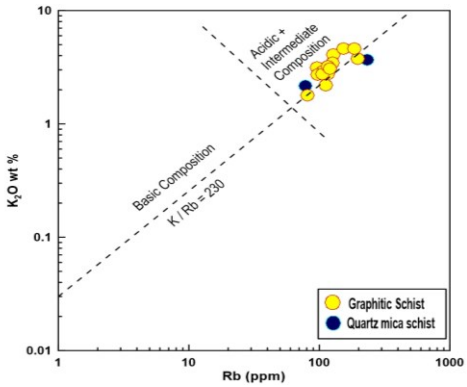

Fig.11 b) K_2O (wt. %) versus Rb (ppm) bivariate diagram (after Floyd and Leveridge, 1987, Floyd et.al., 1989). (The magmatic lineage or 'main trend' with the ratio of K/Rb = 230 is after Shaw, 1968)

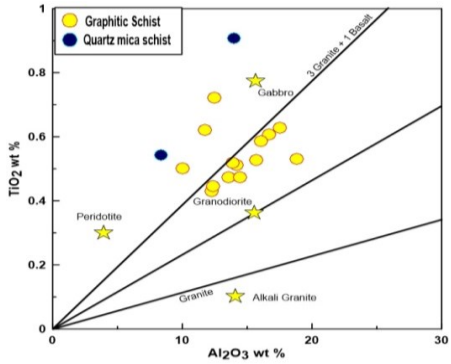

Fig. 11 c) TiO_2 (wt %) versus Al_2O_3 (wt. %) bivariate diagram (after McLennan, Fryer and Young, 1979).

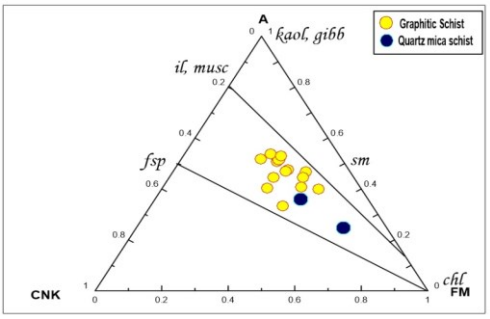

Fig. 11d). A-CNK-FM diagram after Nesbitt and Young (1989) (Mineral abbreviations: kaol, kaolinite; gibb, gibbsite; chl, chlorite; sm, smectite; il, illite; kfsp, potash feldspar; pl, plagioclase. musc, muscovite and fsp, feldspars.)

The different magmatic sources i.e., felsic, intermediate and mafic can be appreciably differentiated using the TiO_2/Zr weight ratio. Hayashi et al. (1997) defined that TiO_2/Zr weight ratio generally has a negative correlation with SiO_2, whose value is > 200 for mafic igneous rocks, 195-55 for inter-mediate igneous rocks and < 55 for felsic rocks. The samples from the present study plotted well within the field of felsic igneous rocks (Fig. 11a). The similar inference of acidic to intermediate precursor of magmatic linage for the meta-sediments of the present study was derived from the widely accepted LILEs (Fig. 11b) based on K_2O (wt. %) and Rb (ppm) bivariate plot (Floyd and Leveridge, 1987; Floyd et al., 1989). The Hayashi et al. (1997) suggested that Al_2O_3 / TiO_2 ratios within fluvially transported detrital siliciclastic sedimentary rocks are concurrent with its magmatic precursor. The felsic source has the value for Al_2O_3 / TiO_2 >21 whereas the mafic is defined by a range of 3 to 8 and the intermediate source lies in between. The sample values for Al_2O_3 / TiO_2 vary from 15.39 to 35.47 with an average of 25.32 and are actually concomitant with

our earlier inference of felsic to intermediate precursor with a mixed source composition. This inference is further amplified by quantification of calculated SiO_2 contents within the theoretically inferred magmatic source of the metasediments. Hayashi et al. (1997) suggested an empirical equation considering relative immobility of aluminum and titanium within the fluvial system and residual weathering of silica content assessment of the probable source rock for siliciclastic sediments. The equation is defined as,

$$SiO_2 \text{ (wt. \%)} = 39.34 + 1.2578\ (Al_2O_3/TiO_2) - 0.0109\ (Al_2O_3/TiO_2)^2$$

The calculated silica content of the samples of the Sonaghati Formation ranges from 56.11 to 70.24 with an average of 63.84, which substantiate the mixed source precursor with acidic and mafic components. Later on, owing to low solubility of Al and Ti oxides and hydroxides in low temperature aqueous solutions, McLennan et al. (1979) proposed a binary plot which can be used as an index of provenance and estimator of the average bulk chemical composition of the source area. These plots also suggest that all the samples of the present study follow the trend falling in between the granodiorite and 3 granite + 1basalt (Fig. 11c)

The source composition of meta-sediments can also be back traced using the CIA values of these samples, which indicate that the speculated precursor varies from granite to granodiorite in composition. The index of ICV can also be utilized for provenance determination since the ICV values for the different magmatic suites are unaffected by the degree of weathering (Cox et al., 1995). The dominance of rock forming minerals i.e., K-feldspars, plagioclase, pyroxenes and amphiboles is indicated by ICV value > 0.84, whereas the dominance of alteration products such as kaolinite, illite, and muscovite is denoted by the ICV values < 0.84 (Cox et al., 1995; Cullers, 2000). The average ICV value for the metasediments of Sonaghati Formation is 1.43, hence the dominance of rock forming minerals is further confirmed.

Cox et al., (1995) had also established the existence of an inverse relationship between ICV and CIA, and had also validated that the clastic sedimentary rocks derived from the variable precursor have different ICV values even after witnessing the same degree of weathering (as reflected by same CIA). The unaltered basalt and granite yield strongly contrasting ICV values of 2.20 and 0.95 (Cox et al., 1995). The ICV values for samples from the present study area ranges from 0.90 to 3.22 with an average of 1.43 a mixed source precursor of metasediments of the present study area. The plot of all the samples on A-CNK-FM diagram i.e.,

$$Al_2O_3\text{-}(CaO+Na_2O+K_2O) - (Fe_2O_3(T)+MgO)$$

after Nesbitt and Young (1989) (Fig. 11a) show most of the samples plot along a mixing line between illite-muscovite and chlorite compositions in contrast to the trend of recent weathering profiles (Fig. 11d). The mixing trend between chlorite and muscovite-illite indicates the presence of mafic rocks in the provenance and also the metasomatic introduction of K_2O during alteration. The LREE enriched and fractionated pattern of these of metasediments also corroborates with the inference of mixed source protolith (McLennan et al., 1984). The contemporary probable source rocks from the vicinity may include Amgaon, Tirodi and Betul basement gneisses, granites, amphibolies and basic dykes and Betul rhyolites.

The provenance characterization can also be carried out using the ratio of transitional elements i.e., Cr and Ni. The dominance of felsic rocks within the provenance is indicated by low Cr and Ni contents and vice versa is for mafic to ultramafic rocks (Condie, 1991; Armstrong-Altrin et al., 2004). The average Cr/Ni ratio ranges from 1.42 to 4.05 with an average of 2.20 thus eventually confirms the mixed source with both the basic and intermediate to felsic precursors.

The results indicate that all these meta-sediments are immature, arkosic sediments having the composition very similar of NASC and the average shale derived from the mixing of felsic, intermediate and mafic magmatic end members. But the dominant contributor for this formation is acidic and intermediate precursor, with small fraction of mafic component.

Paleoclimate

The palaeo-redox conditions during sedimentation of siliciclastic rocks can also be evaluated from their chemistry. The oxygen fugacity, humidity, CO_2 concentration, biological productivity, etc. are the key factors which influence the whole rock chemistry of any sedimentary succession either of present or past. Therefore, detailed study of weathering index of ancient sediments provides useful inferences on past climate. The binary plot of SiO_2 wt. % versus ($Al_2O_3 + K_2O + Na_2O$) wt. % proposed by Suttner and Dutta (1986) indicates that analysed samples plot in the field of semi arid climate (Fig. 12) but shows a sequential variation, suggesting that they were deposited under variable climatic conditions ranging from semi-arid to arid. According to Hallberg (1976); the values of Cu/Zn ratio are considered as an indicator of palaeo-redox conditions, the high values of Cu/Zn ratio indicate reducing conditions, while their lower values suggest oxidizing conditions. The Cu/ Zn ratio of all the samples is high (greater than 0.75) except the QMS (0.18), and the V/Cr ratio of GS samples varies from 1.97 to 3.71 with an average of 2.8 and for QMS samples it varies from 1.6 to 1.7. Similarly V/Cr ratio could also be used as a Paleoclimate proxy. The

reducing environment is suggested by value greater than 2 whereas the reverse is true for value lower than 2 (Jones and Manning, 1994).

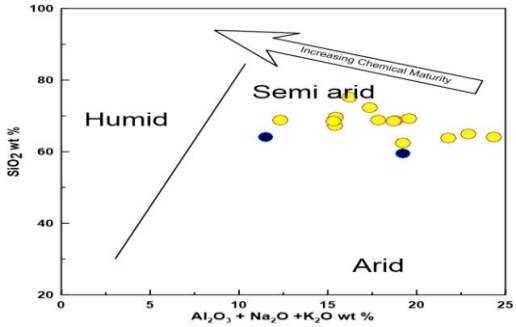

Fig. 12 Bivariate SiO_2 (wt. %) versus Al_2O_3 + K_2O + Na_2O (wt. %) Paleoclimate discrimination diagram. Fields after Suttner and Dutta (1986).

The high values of Cu/Zn and V/Cr ratio suggest that these fine clastics were deposited under reducing conditions. The presence of pyrite in the form of disseminations, specks and stringers along and across the foliation planes (Fig. 13) also supports the reducing environment of crystallization.

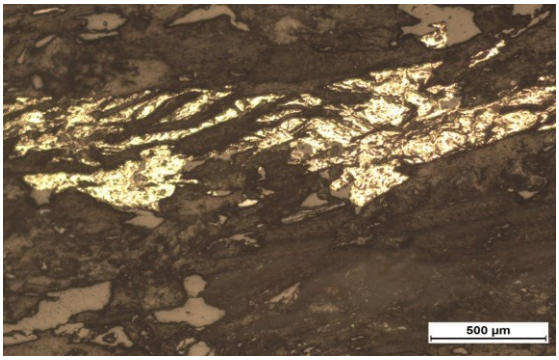

Fig.13: Photomicrograph of Quartz Mica Schist from borehole no. BBT-1 showing Pyrite occupying the interstitial spaces of the ground mass and also present as specks.

Summary & Conclusions

The schematic geochemical characterization of metasediments of Sonaghati Formation, Betul belt, from Tikari-Gauthana-Chiklar area Betul District, Madhya Pradesh was attempted with the aptitude for utilizing the geochemical analogy for provenance delineation and plaeo-climatic reconstruction.

From the meta-sedimentary rocks including Quartz Mica Schist and Graphite Schist sixteen core samples were randomly selected from varying depth for geochemical characterization of these metasediments. These metasediments are fine grained with equigranular hypidiomorphic texture. The dominant minerals are muscovite, quartz and opaques (±graphite/Fe-Ti oxides) whereas chlorite, k feldspar, plagioclase, biotite, hornblend and diopside (±Kyanite & ± andalusite) occur in minor amounts with varying proportion within the samples. The schistosity is well developed and defined by parallel alignment of flaky graphite, biotite and muscovite. The shearing is evidenced by pinch & swell structure, mica fish and sigmoidal prophyroblasts. The Bivariate XY plots of Major Oxides versus Silica displays a moderate to strong negative correlation between silica and all the other major oxides except the outlier samples for CaO. The collinear trends in the XY plots indicate that the sediments belong to single / related population and the visible compositional variation could be attributed to chemical, mineralogical and textural maturity. The geochemical signatures were probable governed by the following minerals {quartz, clay minerals, opaque's (Ti-Fe-Mg Oxides) and some mafic minerals}. The strong positive correlation between Al_2O_3 and K_2O, K_2O and Na_2O also suggests the dominance of clay minerals. The CIA value varies between 55.2 and 77.8 with an average of 69.3 and is comparable with the average CIA values for global shale (~ 70 to ~ 75) given. This also implies the presence of muscovite, illites and smectite within the samples of metasediments of Sonaghati Formation. The co-linear trends among the Compatible and High Field Strength Elements further suggests that the data set belongs to a single/ related population, eventually uninfluenced by the secondary process of chemical alterations and preserving the primordial elemental signatures.

The samples of metasediments from Songhati Formation have an enriched REE pattern with negative Eu anomaly. This fractionated LREE's dispersal with nearly flat and enriched HREE's on Chondrite normalized REE plot implies that Sonaghati meta-sediment have a mixed source protolith. The presence of strong negative Eu anomaly further affirms with the Proterozoic age for the precursor of the metasediments. The Overall abundance of Rare Earth Elements in these meta-sediments is comparable with the North American Shale Composite (NASC) with very slight depletion in HREE's.

The Geochemical signatures of the metasediments indicates that these meta-sediments are immature, arksosic sediments having the composition very similar of NASC and the average shale and had witnessed substantial weathering of the source terrain without any evidence of potash metasomatism. It can be further concluded that these were derived from the mixing of felsic, intermediate and mafic magmatic end members but the dominant contributor being the acidic and intermediate precursor, with small fraction of mafic component. The Major Oxide relations also suggest that these sediments were deposited under variable climatic conditions ranging from semi-arid to arid. Cu/Zn , V/Cr ratios and presence of pyrites, graphites suggest that

these fine clastics were deposited under reducing conditions.

Acknowledgement

The assignment was executed as a part of G2 Stage General Exploration for graphite in Tikari-Gauthana- Chiklar and surrounding areas, Betul Disrict, M.P under item No. 068/ME/CR/MP/2015/048, Field Season 2015-16 of Geological Survey of India, Ministry of Mines. The authors gratefully acknowledge Director General, Geological Survey of India, Additional Director General and HOD, Geological Survey of India, Central Region, for providing necessary facilities, technical, administrative and financial for successful completion of the research. The authors are also thankful to Mineral Physics Lab, Nagpur and Chemical Lab, Nagpur, Hyderabad and Bhopal for sample analysis and all the administrative and support system staff for their direct & indirect efforts in bringing up of this manuscript. The authors also express kind acknowledgement towards the expert reviewer for their keen scrutiny and valuable comments for betterment of the manuscript. The competent authorities of GSI are also dully acknowledged for giving necessary approval for publication of this manuscript.

References

Alam, M., Naushad, M., Wanjari, N., Ahmad, T. (2009). Geochemical characterizations of mafic magmatic rocks of the Central Indian Shield: Implication for Precambrian crustal evolution, in Talat Ahmad, Francis Hirsch, and Punya Charusiri (eds.), Journal of the Virtual Explorer, 32, paper 8, doi: 10.3809/jvirtex.2009.00246.

Armstrong-Altrin, J. S., Lee, Y. I., Verma, S. P., & Ramasamy, S. (2004). Geochemistry of sandstones from the upper Miocene Kudankulam Formation, southern India: Implications for provenance, weathering, and tectonic setting. Journal of Sedimentary Research, 74(2), 285–297.

Chakraborty, S.K., Chore, S.A., Vishwakarma, L.L. (2009). Report on the geological studies of the volcano-sedimentary lithoassemblage of Betul belt, Central Indian Tectonic Zone, M.P GSI, Unpublished final report for FS 2000-01 & 2001-02 of Geological Survey on India.

Condie, K.C., Wilks, M., Rosen, D.M., and Zlobin, V.L. (1991). Geochemistry of metasediments from the Precambrian Hapschan Series, eastern Anabar Shield, Siberia. Precambrian Research, 50, 37-47.

Cox, R., Low, D. R., & Cullers, R. L. (1995). The influence of sediment recycling and basement composition on evolution of mud rock chemistry in the south-western United States. Geochimica et Cosmochimica Acta, 59, 2919 – 2940.

Cullers, R. L. (2000). The geochemistry of shales, siltstones, and sandstones of Pennsylvanian-Permian age Colorado, U.S.A.: Implications for provenance and metamorphic studies. Lithos, 51, 181–203.

Dar S. A., Khan K. F., & Mir A. R. (2020). Provenance and paleo-weathering of Paleoproterozoic siliciclastic sedimentary rocks of Bijawar Group, Sonrai Basin, Uttar Pradesh, India: using a geochemical approach. Journal of Sedimentary Environments, https://doi.org/10.1007/s43217-020-00024-5.

Eswaran, H., Stoops, G., D Paepe, R. (1973). A Contribution to the study of soil formation of Isla Santa Cruz Galapegose. Pedologie, 23, 100-122.

Fedo, C.M. Eriksson, K.A., Krogstad, E.J. (1996). Geochemistry of shales from the Archean (~ 3.0ga) Buhwa Greenstone Belt, Zimbabwe: Implecations for provenance and source-area weathering. Geochimica et Cosmochimica Acta , 60, 1751-1763.

Fedo, C.M., Nesbitt, H.W., & Young, G.M. (1995). Unrevalling the effects of Potassium metasomatism in the sedimentary rocks and paleosols with implications for paleoweathering conditions and provenance. Geology, 23, 921-924.

Floyd, P.A. and Leveridge, B.E. (1987). Tectonic environment of the Devonian Gramscatho basin, south Cornwall: framework mode and geochemical evidence from turbidite sandstones. Journal of the Geological Society of London, 144, 531–542.

Floyd, P.A., Winchester, J.A., and Park R.G. (1989). Geochemistry and Tectonic Setting of Lewisian Clastic Metasediments from the Early Proterozoic Loch Maree Group of Gairloch, NW Scotland. Precambrian Research, 45, 203-214.

Garrels, R.M., Mackenzie, F.T. (1971). The Evolution of Sedimentary Rocks. W.W. Norton, New York.

Gibbs, A. K., Montgomery, C. W., O'day, P. A. and Erslev E. A. (1986). The Archean-Proterozoic transition: Evidence from the geochemistry of metasedimentary rocks of Guyana and Montana. Geochimica et Cosmochimica Acta, 50, 2125-2141.

Gilboy, C.F. (1982). Classification of Clastic metasediments. Saskatchewan Mineral resources, Open File report 82-3, 33 p.

Gracia, D., Fonteilles, M., and Moutte, J. (1994). Sedimentary Fractionations between Al, Ti, and Zr and the Genesis of Strongly Peraluminous Granites. The Journal of Geology, 102 (4), 411-422.

Gromet, L.P., Dymek, R.F., Haskin, L.A., and Korotev, R.L. (1984). "The North American shale composite'': its compilation, major and trace element characteristics. Geochimica et Cosmochimica Acta, 48, 2469–3482.

GSI, Bulletin series A-69, (2018). Zinc- Copper Mineralization of Betul Belt, Betul and Chhindwara districts Madhya Pradesh (2018). Bulletin series A, No.69, Geological Survey of India, Nagpur, ISSN 0536-8782.

Hallberg, R.O. (1976). A geochemical method for investigation of palaeoredox conditions in sediments. Ambio, 4, 139–147, Special Report.

Hamdam, J., and Bumham, C.P. (1996). The contribution of nutrients from the parent material in three deeply weathered soils of Peninsular Malaysia. Geoderma, 74, 219-233.

Harnois, L. (1988). The CIW index: a new chemical Inex of weathering. Sedimentary Geology, 55, 319-322.

Hayashi, K.I., Fujisawa, H., Holland, H.D., and Ohomoto, H. (1997). Geochemistry of ~ 1.9 Ga sedimentary rocks from northern Labrador, Canada. Geochim Cosmochim Acta, 61 (19), 4115–4137.

Heinrichs, T., Siegesmund, S., Frei, D., Drobe, M., and Schulz, B. (2012). Provenance signatures from whole-rock geochemistry and detrital zircon ages of metasediments from the Austroalpine basement south of the Tauern Window (Eastern Tyrol, Austria). Geo. Alp, 9, 156–185.

Herron, M. M. (1988). Geochemical classification of terrigenous sands and shales from core or log data: Journal of Sedimentary Petrology, 58(5), 820- 829.

Jones, B. and Manning, D.C. (1994). Comparison of geochemical indices used for the interpretation of paleo-redox conditions in Ancient mudstones. Chemical Geology, 111(1-4), 111-129.

Lenka, B. (2014). Investigation for graphite in Tikari-Gauthana-Chiklar and surrounding area, Betul district, M.P (G3 stage). Unpublished final report of Geological Survey on India for FS-2013-14. Accession No CR-023185.

Lenka, B. and Ahmad, A. (2013): Investigation for graphite in Tikari, Chiklar, Gauthana area, Betul district, M.P. Unpublished final report of Geological Survey on India for FS-2012-13. Accession No 22887, pp. 92.

Lenka.B and Shukla, S. (2016). General Exploration For Graphite in Tikari- Gauthana- Chiklar and surrounding areas, Betul district, M.P (G2 Stage). Unpublished final report of Geological Survey on India for FS-2015-16. Accession No CR-023185.

Maynard, J.B., Sutton,S.J., Robb, L.J., Ferraz, M.F., and Meyer, F.M. (1995). A paleosol developed on hydrothermally altered granite from the hinterland of the Witwaterrand basin: characteristics of a source of basn fill. Journal of Geology,103, 357-377.

Mclennan, S.M., Fryer, B.J., Young, G.M. (1979). The geochemistry of the carbonate-rich Espanola Formation (Huronian) with emphasis on the rare earth elements. Canadian Journal of Earth Sciences, 16, 230-239.

McLennan, S.M., Hemming, S., McDaniel, D.K., and Hanson, G.N. (1993). Geochemical approaches to sedimentation, provenance and tectonics, in Johnsson, M.J., Basu, A. (Eds.), Processes Controlling the Composition of Clastic Sediments. Geological Society of America Special Paper 284., Boulder, Colorado, p. 21–40.

Mclennan, S.M., Taylor S. R. and Mcgregdr, V. R. (1984). Geochemistry of Archean metasedimentary rocks from West Greenland. Geochimica et Cosmochimica Acta, 48, 1-13.

Mishra, M.K., Devi, S.J., Kaulina, T., Dass, K.C., Kumar, S. and Ahmad, T. (2011). Petrogenesis and tectonic setting of the Proterozoic mafic magmatic rocks of the Central Indian Tectonic Zone, Betul Area: Geochemical Constraints. in Srivastava, R.K. (Ed.), Dyke Swarms: Keys for Geodynamic Interpretation, Berlin Heidelberg: Springer-Verlag, p. 189-201.

Nesbitt, H.W. and Young, G.M. (1989). Formation and diagenesis of weathering profiles. Journal of Geology, 97, 129–147.

Nesbitt, H.W., & Young, G.M. (1982). Early Proterozoic climates and plate motions inferred from major element chemistry of lutites. Nature, 299, 715–717.

Nesbitt, H.W., & Young, G.M. (1984). Prediction of some weathering trends of plutonic and volcanic rocks based on thermodynamic and kinetic considerations. Geochim Cosmochim Acta, 48, 1523–1534.

Parker, A. (1970). An index of weathering for Silicate rocks. Geological Magazine, 107, 501-504.

Pettijohn, F. J. (1963). Chemical composition of sandstones—excluding carbonate and volcanic sands, in Fleischer, M., ed., Data of Geochemistry, sixth edition, U. S. Geological Survey Professional Paper 440-S, 21 p.

Praveen M.N. (2016). Geochemistry and petrogenesis of rhyolites hosting VMS mineralization in the eastern Betul belt, Central India. PhD thesis submitted to the Cochin University of Science and Technology, Cochin.

Prince J. R. & Velbel M. A. (2003) Chemical weathering indices applied to weathering profiles developed on heterogeneous felsic metamorphic parent rocks. Chemical Geology, 202, 397-416.

Raut, P.K., Mahakud, S.P. (2002). Geology, geochemistry and tectonic setting of volcano-sedimentary sequence of Betul belt, Madhya Pradesh and ore genesis of related Zinc and Copper sulphide mineralization. Proceedings of the National Seminar on Mineral Exploration and Resource Surveys, by Geological Survey of India, held at Jaipur.

Roy, A., and Prasad, H.M. (2003). Tectonothermal events in Central Indian Tectonic Zone (CITZ) and its implications in Rodinian crustal assembly. Journal of Asian Earth Sciences, 22, 115–129.

Sarkar, S.N., Trivedi, J.R., Gopalan, K., (1986). Rb–Sr whole rock and mineral isochron age of the Tirodi gneiss, Sausar Group, Bhandara district, Maharashtra. Journal of Geological Society of India, 27, 30 – 37.

Sawyer, E.W. (1986). The influence of source rock type, chemical weathering and sorting on the geochemistry of clastic sediments from the Quetico Meta-sedimentary belt, Superior Province, Canada. Chemical Geology 55, 77-95.

Shaw, D. M. (1968). A review of K-Rb fractionation trends by covariance analysis. Geochimica et Cosmochimica Acta, 32, 573-602.

Srivastava, S.K and Chellani, S.K. (1995). Report on Special thematic mapping of Archean Proterozoic rocks in area north of Bordehi & around Khari Betul dist.,M.P, Unpublished final report of Geological Survey on India for FS-1994-1995. Accession No CR-021502.

SOP (2010). Standard procedure of sample processing for petrochemical analysis of Geological Survey of India. www.gsi.gov.in.

Suttner, L.J. and Dutta, P.K. (1986). Alluvial sandstone composition and palaeoclimate Framework mineralogy. Journal of Sedimentary Petrology, 56(3), 329–345.

Taylor, S.R. and McLennan, S.M. (1985). The Continental Crust: Its Composition and Evolution. Oxford, Blackwell, p. 311.

Wronkiewicz, D.J. and Condie, K.C. (1987). Geochemistry of Archean shales from the Witwatersrand Supergroup, South Africa: Source-area weathering and provenance. Geochimica et Cosmochimica Acta, 51, 2401-2416.

Yousuf, I., Subba Rao, D.V., Balakrishnan, S., and Ahmad, T. (2019). Geochemistry and petrogenesis of acidic volcanics from Betul–Chhindwara Belt, Central Indian Tectonic Zone (CITZ), Central India. Journal of Earth System Sciences, 128, 227.

(Received on 16 February, 2021; Revised Accepted on 3 May 2021)